

Finite-time stabilisation of cyclic formations using bearing-only measurements

Shiyu Zhao^a, Feng Lin^b, Kemao Peng^b, Ben M. Chen^{c,*} and Tong H. Lee^c

^aGraduate School for Integrative Sciences and Engineering, National University of Singapore, Singapore; ^bTemasek Laboratories, National University of Singapore, Singapore; ^cDepartment of Electrical and Computer Engineering, National University of Singapore, Singapore

(Received 10 January 2013; accepted 7 October 2013)

This paper studies decentralised formation control of multiple vehicles in the plane when each vehicle can only measure the local bearings of their neighbours by using bearing-only sensors. Since the inter-vehicle distance cannot be measured, the target formation involves no distance constraints. More specifically, the target formation considered in this paper is an angle-constrained cyclic formation, where each vehicle has exactly two neighbours and the angle at each vehicle subtended by its two neighbours is pre-specified. To stabilise the target formation, we propose a discontinuous control law that only requires the sign information of the angle errors. Due to the discontinuity of the proposed control law, the stability of the closed-loop system is analysed by employing a locally Lipschitz Lyapunov function and nonsmooth analysis tools. We prove that the target formation is locally finite-time stable with collision avoidance guaranteed.

Keywords: formation control; bearing-only measurement; discontinuous dynamic system; finite-time stability

1. Introduction

In the existing work on multi-vehicle formation control, it is commonly assumed that each vehicle can obtain the positions of their neighbours (Dimarogonas & Johansson, 2010; Hu, Xu, & Xie, 2013; Keller et al., 2013; Kopeikin, Ponda, Johnson, & How, 2013; Lin, Francis, & Maggiore, 2005; Ren & Cao, 2011; Tian & Wang, 2013). It is notable that *position* information essentially consists of two kinds of partial information: *bearing* and *distance*. In recent years, formation control using bearing-only (Basiri, Bishop, & Jensfelt, 2010; Eren, 2012; Franchi & Giordano, 2012; Moshtagh, Michael, Jadbabaie, & Daniilidis, 2008) or distance-only (Cao, Yu, & Anderson, 2011) measurements has attracted some attention. In this paper, we will investigate *formation control using bearing-only measurements* (or called *bearing-based formation control*). We assume that each vehicle can only measure the bearings of their neighbours and inter-vehicle distances are unavailable. In practical applications, bearings can be conveniently measured by using monocular cameras, which are very common sensors nowadays. A camera inherently is a bearing-only sensor. As long as the target can be localised in the image, the bearing of the target relative to the camera can be easily calculated based on the pin-hole camera model (Ma, Soatto, Kosecka, & Sastry, 2004, Section 3.3). Hence vision-based cooperative control tasks (Das et al., 2002; Mariottini et al., 2009) are the potential applications of the research on bearing-based formation control.

A number of interesting and challenging problems arise when only bearings are available for formation control. One key problem is how to utilise the bearing measurements for formation control. There are generally two approaches. The first approach is to implement control laws directly using bearing measurements; the second approach is to estimate vehicle positions using bearing measurements, and then implement formation control laws based on the estimated positions. In this paper, we will adopt the first approach. The reason we do not use the second approach is that position estimation using bearings requires certain observability conditions. For example, suppose vehicle A is stationary and vehicle B can measure the bearings of vehicle A from two different angles. Then vehicle A can be localised as the intersection of the two bearings measured by vehicle B. However if vehicle B is only able to measure vehicle A from one single angle, the distance between the two vehicles is impossible to be recovered. In other words, relative motions between vehicles are fundamentally necessary for position estimation using bearing measurements. However, in many formation control tasks, the relative positions of the vehicles in the formation are required to be stationary, and hence the observability condition is not satisfied.

If each vehicle is controlled based on bearings only, the inter-vehicle distance in the formation would be uncontrollable. As a result, any bearing-based formation control law can only stabilise *bearing-constrained* target formations. The term bearing-constrained as used here refers to

*Corresponding author. Email: bmchen@nus.edu.sg

the bearings of the edges connecting vehicles or the angles at each vehicle subtended by their neighbours are constrained. Another challenging problem is collision avoidance, which is important for all kinds of formation control problems. Collision avoidance is particularly important for bearing-based formation control as inter-vehicle distances are unmeasurable and uncontrollable. To make any bearing-based formation control law practically applicable, we need to guarantee collision avoidance between any vehicles no matter they are neighbours or not.

As a relatively new research topic, bearing-based formation control has not been completely solved yet. Only a few special cases have been analysed in the literature. Moshtagh et al. (2008) proposed a distributed control law for balanced circular formations of unit-speed vehicles. The proposed control law can globally stabilise balanced circular formations using bearing-only measurements. Basiri et al. (2010) studied distributed control of triangular formations of three vehicles using bearing-only measurements. The global stability of the proposed formation control law is proved by employing the Poincaré–Bendixson theorem. However, the Poincaré–Bendixson theorem is only applicable to the scenarios involving only three or four vehicles. Eren (2012) investigated formation shape control using bearing measurements. Bearing rigidity is proposed to formulate bearing-based formation control problems. A bearing-based control law is designed for a formation of three non-holonomic vehicles. Bishop (2011) proposed a control law that can stabilise general bearing-constrained formations. However, the proposed control law in Bishop (2011) still requires position measurements. Based on the concept of parallel rigidity, Franchi and Giordano (2012) proposed a distributed control law to stabilise bearing-constrained formations using bearing-only measurements. However, the proposed control law in Franchi and Giordano (2012) requires communications among the vehicles. That is different from the problem considered in this paper, where we assume there are no communications between any vehicles and each vehicle cannot share their bearing measurements with their neighbours.

In this paper, we study distributed bearing-based control of cyclic formations in the plane. The sensing graph of the formation is an undirected cycle with fixed topology. In the target formation, the angle at each vehicle subtended by its two neighbours is constrained. For cyclic formations, the angle constraints cannot specify a unique formation shape. To well define a formation shape using angle constraints, we may assign more complicated underlying graphs such as rigid graphs to the formation. However, we only consider cycle graphs in this paper and leave more complicated cases for future research. The main contributions of this work are summarised as follows:

- (1) To stabilise angle-constrained cyclic formations, we propose a distributed discontinuous control law

that only requires the sign information of the angle errors. Compared to the existing work in Basiri et al. (2010), our control law is able to stabilise cyclic formations with an arbitrary number of vehicles. In addition, this work requires no parallel rigidity assumptions (Bishop, 2011; Eren, 2012) on the target formation.

- (2) Finite-time control has attracted much attention in recent years (Chen, Lewis, & Xie, 2011; Hong, Jiang, & Feng, 2010; Hong, Xu, & Huang, 2002; Meng & Lin, 2012; Xiao, Wang, Chen, & Gao, 2009). Besides fast convergence, finite-time control can also bring benefits such as disturbance rejection and robustness against uncertainties (Bhat & Bernstein, 2000). In this paper, we prove the proposed control law ensures local finite-time convergence of the angle errors. The finite-time stability of the nonlinear closed-loop system is proved by using nonsmooth analysis tools (Bacciotti & Ceragioli, 1999; Clarke, 1983; Cortés, 2008; Cortés & Bullo, 2005; Filippov, 1988; Paden & Sastry, 1987).
- (3) Collision avoidance is a particularly important issue for bearing-based formation control as inter-vehicle distances are unmeasurable. We prove that the proposed control law guarantees collision avoidance between any vehicles (no matter they are neighbours or not) given sufficiently small initial angle errors.

The paper is organised as follows. Preliminaries to graph theory and nonsmooth analysis are introduced in Section 2. Section 3 presents the problem formulation and the proposed control law. The formation stability by the proposed control law is proved in Section 4. Section 5 shows simulation results to verify the theoretical analysis. Conclusions are drawn in Section 6.

2. Preliminaries to graph theory and nonsmooth analysis

2.1 Notations

Given a symmetric positive semi-definite matrix $A \in \mathbb{R}^{n \times n}$, the eigenvalues of A are denoted as $0 \leq \lambda_1(A) \leq \lambda_2(A) \leq \dots \leq \lambda_n(A)$. Let $\mathbf{1} = [1, \dots, 1]^T \in \mathbb{R}^n$, and I be the identity matrix with appropriate dimensions. Denote $|\cdot|$ as the absolute value of a real number, and $\|\cdot\|$ as the Euclidean norm of a vector. Denote $\text{Null}(\cdot)$ as the right null space of a matrix. Let $[\cdot]_{ij}$ be the entry at the i th row and j th column of a matrix, and $[\cdot]_i$ be the i th entry of a vector. Given a set S , denote \bar{S} as its closure. For any angle $\alpha \in \mathbb{R}$,

$$R(\alpha) = \begin{bmatrix} \cos \alpha & -\sin \alpha \\ \sin \alpha & \cos \alpha \end{bmatrix} \in \mathbb{R}^{2 \times 2} \quad (1)$$

is a rotation matrix satisfying $R^{-1}(\alpha) = R^T(\alpha) = R(-\alpha)$. Geometrically, $R(\alpha)$ rotates a vector in \mathbb{R}^2 counterclockwise through an angle α about the origin.

2.2 Graph theory

A graph $\mathcal{G} = (\mathcal{V}, \mathcal{E})$ consists of a vertex set $\mathcal{V} = \{1, \dots, n\}$ and an edge set $\mathcal{E} \subseteq \mathcal{V} \times \mathcal{V}$. If $(i, j) \in \mathcal{E}$, then i and j are called to be adjacent. The set of neighbours of vertex i is denoted as $\mathcal{N}_i = \{j \in \mathcal{V} \mid (i, j) \in \mathcal{E}\}$. A graph is undirected, if each $(i, j) \in \mathcal{E}$ implies $(j, i) \in \mathcal{E}$, otherwise the graph is directed. A path from i to j in a graph is a sequence of distinct nodes starting with i and ending with j such that consecutive vertices are adjacent. If there is a path between any two vertices of graph \mathcal{G} , then \mathcal{G} is said to be connected. An undirected cycle graph is a connected graph where every vertex has exactly two neighbours.

An incidence matrix of a directed graph is a matrix E with rows indexed by edges and columns indexed by vertices.¹ Suppose (j, k) is the i th edge. Then the entry of E in the i th row and k th column is 1, the one in the i th row and j th column is -1 , and the others in the i th row are 0. By definition, we have $E\mathbf{1} = 0$. If a graph is connected, the corresponding E has rank $n - 1$ (see (Godsil & Royle, 2001, Theorem 8.3.1)). Then $\text{Null}(E) = \text{span}\{\mathbf{1}\}$.

2.3 Nonsmooth stability analysis

Next we introduce some useful concepts and facts regarding discontinuous dynamic systems (Bacciotti & Ceragioli, 1999; Clarke, 1983; Cortés, 2008; Cortés & Bullo, 2005; Filippov, 1988; Paden & Sastry, 1987).

2.3.1 Filippov differential inclusion

Consider the dynamic system,

$$\dot{x}(t) = f(x(t)), \tag{2}$$

where $f : \mathbb{R}^n \rightarrow \mathbb{R}^n$ is a measurable and essentially locally bounded function. The Filippov differential inclusion (Filippov, 1988) associated with the system (2) is

$$\dot{x} \in \mathcal{F}[f](x), \tag{3}$$

where $\mathcal{F}[f] : \mathbb{R}^n \rightarrow 2^{\mathbb{R}^n}$ is defined by

$$\mathcal{F}[f](x) = \bigcap_{r>0} \bigcap_{\mu(S)=0} \overline{\text{co}}\{f(B(x, r) \setminus S)\}. \tag{4}$$

In Equation (4), $\overline{\text{co}}$ denotes convex closure, $B(x, r)$ denotes the open ball centred at x with radius $r > 0$, and $\mu(S) = 0$ means that the Lebesgue measure of the set S is 0. The set-valued map $\mathcal{F}[f]$ associates each point x with a set. Note $\mathcal{F}[f](x)$ is multiple valued only if $f(x)$ is discontinuous at x .

A Filippov solution of Equation (2) on $[0, t_1] \subset \mathbb{R}$ is defined as an absolutely continuous function $x : [0, t_1] \rightarrow \mathbb{R}^n$ that satisfies Equation (3) for almost all $t \in [0, t_1]$. If $f(x)$ is measurable and essentially locally bounded, the existence of Filippov solutions can be guaranteed (Cortés & Bullo 2005, Lemma 2.5; Cortés 2008, Proposition 3), though the uniqueness cannot. The interested reader is referred to (Cortés, 2008, p. 52) for the uniqueness conditions of Filippov solutions. A solution is called maximal, if it cannot be extended forward in time. A set Ω is said to be weakly invariant (respectively strongly invariant) for Equation (2), if for each $x(0) \in \Omega$, Ω contains at least one maximal solution (respectively all maximal solutions) of Equation (2).

2.3.2 Generalised gradient

Suppose $V : \mathbb{R}^n \rightarrow \mathbb{R}$ is a locally Lipschitz function. If $V(x)$ is differentiable at x , denote $\nabla V(x)$ as the gradient of $V(x)$ with respect to x . Let M_V be the set where $V(x)$ fails to be differentiable. The generalised gradient (Clarke, 1983; Cortés, 2008; Cortés & Bullo, 2005) of $V(x)$ is defined as

$$\partial V(x) = \text{co} \left\{ \lim_{i \rightarrow +\infty} \nabla V(x_i) \mid x_i \rightarrow x, x_i \notin S \cup M_V \right\},$$

where co denotes convex hull and S is an arbitrary set of Lebesgue measure zero. The generalised gradient is a set-valued map. If $V(x)$ is continuously differentiable at x , then $\partial V(x) = \{\nabla V(x)\}$.

Given any set $S \subseteq \mathbb{R}^n$, let $\text{Ln} : 2^{\mathbb{R}^n} \rightarrow 2^{\mathbb{R}^n}$ be the set-valued map that associates S with the set of least-norm elements of \overline{S} . If S is convex, $\text{Ln}(S)$ is singleton. In this paper, we only apply Ln to generalised gradients, which are always convex. For a locally Lipschitz function $V(x)$, $\text{Ln}(\partial V) : \mathbb{R}^n \rightarrow \mathbb{R}^n$ is called the generalised gradient vector field. The following fact (Cortés, 2008, Proposition 8)

$$\mathcal{F}[\text{Ln}(\partial V(x))] = \partial V(x) \tag{5}$$

will be very useful in our work. A point x is called a critical point if $0 \in \partial V(x)$. For a critical point x , it is obvious that $\text{Ln}(\partial V(x)) = \{0\}$.

2.3.3 Set-valued Lie derivative

The evolution of a locally Lipschitz function $V(x)$ along the solutions to the differential inclusion $\dot{x} \in \mathcal{F}[f](x)$ can be characterised by the set-valued Lie derivative (Bacciotti & Ceragioli, 1999; Cortés, 2008; Cortés & Bullo, 2005), which is defined by

$$\begin{aligned} \tilde{\mathcal{L}}_{\mathcal{F}}V(x) &= \{\ell \in \mathbb{R} \mid \exists \xi \in \mathcal{F}[f](x), \\ &\forall \zeta \in \partial V(x), \xi^T \zeta = \ell\}. \end{aligned}$$

With a slight abuse of notation, we also denote $\tilde{\mathcal{L}}_f V(x) = \tilde{\mathcal{L}}_{\mathcal{F}} V(x)$. The set-valued Lie derivative may be empty. When $\tilde{\mathcal{L}}_{\mathcal{F}} V(x) = \emptyset$, we take $\max \tilde{\mathcal{L}}_{\mathcal{F}} V(x) = -\infty$ (see Bacciotti & Ceragioli, 1999; Cortés, 2008; Cortés & Bullo, 2005).

A function $V : \mathbb{R}^n \rightarrow \mathbb{R}$ is called regular (Cortés, 2008, p. 57) at x if the right directional derivative of $V(x)$ at x exists and coincides with the generalised directional derivative of $V(x)$ at x . Note a locally Lipschitz and convex function is regular. The following two lemmas are useful for proving the stability of discontinuous systems using nonsmooth Lyapunov functions. The next result can be found in Shevitz and Paden (1994), Bacciotti and Ceragioli (1999) and Cortés and Bullo (2005).

Lemma 2.1: *Let $V : \mathbb{R}^n \rightarrow \mathbb{R}$ be a locally Lipschitz and regular function. Suppose the initial state is x_0 and let $\Omega(x_0)$ be the connected component of $\{x \in \mathbb{R}^n \mid V(x) \leq V(x_0)\}$ containing x_0 . Assume the set $\Omega(x_0)$ is bounded. If $\max \tilde{\mathcal{L}}_f V(x) \leq 0$ or $\tilde{\mathcal{L}}_f V(x) = \emptyset$ for all $x \in \Omega(x_0)$, then $\Omega(x_0)$ is strongly invariant for Equation (2). Let*

$$Z_{f,V} = \{x \in \mathbb{R}^n \mid 0 \in \tilde{\mathcal{L}}_f V(x)\}. \quad (6)$$

Then any solution of Equation (2) starting from x_0 converges to the largest weakly invariant set M contained in $\bar{Z}_{f,V} \cap \Omega(x_0)$. Furthermore, if the set M is a finite collection of points, then the limit of all solutions starting from x_0 exists and equals one of them.

The next result can be found in Paden and Sastry (1987) and Cortés and Bullo (2005).

Lemma 2.2: *Let $V : \mathbb{R}^n \rightarrow \mathbb{R}$ be a locally Lipschitz and regular function. Suppose the initial state is x_0 and let S be a compact and strongly invariant set for Equation (2). If $\max \tilde{\mathcal{L}}_f V(x) \leq -\kappa < 0$ almost everywhere on $S \setminus Z_{f,V}$, then any solution of Equation (2) starting at $x_0 \in S$ reaches $Z_{f,V} \cap S$ in finite time. The convergence time is upper bounded by $(V(x_0) - \min_{x \in S} V(x))/\kappa$.*

3. Problem formulation

In this section, we first describe the formation control problem that we are going to solve. Then we propose a distributed bearing-based control law and derive the closed-loop system dynamics.

3.1 Control objective

Consider n ($n \geq 3$) vehicles in the plane. Denote the position of vehicle i as $z_i \in \mathbb{R}^2$, $i \in \{1, \dots, n\}$. The dynamics of each vehicle is modelled as

$$\dot{z}_i = u_i,$$

where $u_i \in \mathbb{R}^2$ is the control input to be designed. The target formation considered in this paper is an angle-constrained cyclic formation. The underlying information flow among the vehicles is described by an undirected cycle graph with fixed topology. By indexing the vehicles properly, we can have $\mathcal{N}_i = \{i-1, i+1\}$ for $i \in \{1, \dots, n\}$, which means vehicles $i-1$ and $i+1$ are the neighbours of vehicle i . Then vehicle i can obtain the bearings of vehicles $i-1$ and $i+1$ by using, for example, a monocular camera. Note that the indices $i-1$ and $i+1$ are taken modulo n in this paper. Let $e_i \triangleq z_{i+1} - z_i$. Then the unit-length vector,

$$g_i \triangleq \frac{e_i}{\|e_i\|},$$

characterises the relative bearing between vehicles i and $i+1$ (see Figure 1). Thus the bearing measurements obtained by vehicle i consist of $-g_{i-1}$ and g_i , which are the relative bearings of vehicle $i-1$ and vehicle $i+1$, respectively.

Denote $\theta_i \in [0, 2\pi)$ as the angle subtended by vehicles $i-1$ and $i+1$ at vehicle i . The angle θ_i is specifically defined in the following way: rotating $-g_{i-1}$ counterclockwise through an angle θ_i about vehicle i yields g_i (see Figure 1). This can be mathematically expressed as

$$g_i = R(\theta_i)(-g_{i-1}), \quad (7)$$

where $R(\cdot)$ is the rotation matrix given in Equation (1). By defining θ_i in Equation (7), the angles θ_i and θ_{i+1} are on the same side of edge e_i for all $i \in \{1, \dots, n\}$. As a result, the quantity $\sum_{i=1}^n \theta_i$ is invariant to the positions of the vehicles because the sum of the interior angles of a polygon is constant. Hence $\sum_{i=1}^n \theta_i(t) \equiv \sum_{i=1}^n \theta_i(0)$ for all $t \in [0, +\infty)$. The angle θ_i is specified as a constant

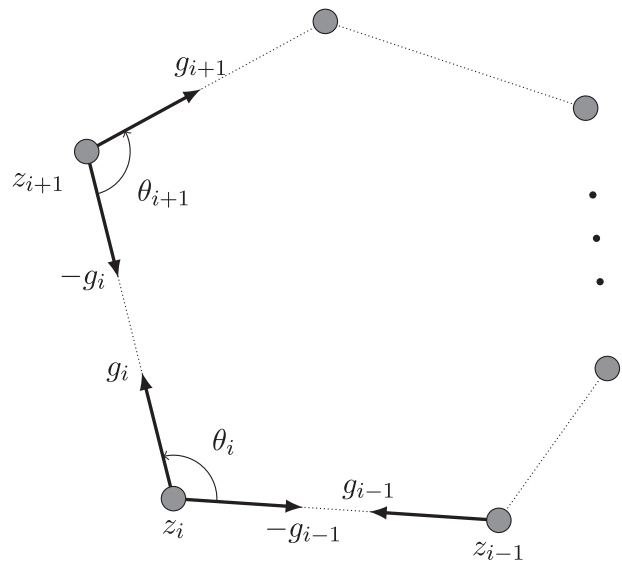


Figure 1. An illustration of cyclic formations.

value $\theta_i^* \in [0, 2\pi)$ in the target formation. The target angles $\{\theta_i^*\}_{i=1}^n$ should be feasible such that there exist formations satisfying the angles constraints.

The problem we investigate in this paper is formally stated as follows:

Assumption 3.1: *In the initial formation, no two vehicles coincide with each other, i.e. $z_i(0) \neq z_j(0)$ for all $i \neq j$.*

Assumption 3.2: *In the target formation, $\theta_i^* \neq 0$ and $\theta_i^* \neq \pi$ for all $i \in \{1, \dots, n\}$.*

Remark 1: Assumption 3.2 means no three consecutive vehicles in the target formation are collinear. The collinear case is a theoretical difficulty in many formation control problems (see, for example, Dörfler & Francis, 2010; Huang, Yu, & Wu, 2013; Krick, Broucke, & Francis, 2009). In practice, bearings are usually measured by optical sensors such as cameras. Hence vehicle i would not be able to measure the bearings of its two neighbours simultaneously when $\theta_i = 0$ due to line-of-sight occlusion. On the other hand, the field-of-view of a monocular camera usually is less than 180° . Hence vehicle i would not be able to measure the bearings of its two neighbours simultaneously when $\theta_i = \pi$ due to limited field-of-view. Thus Assumption 3.2 is reasonable from the practical point of view.

Problem 3.3: Under Assumptions 3.1 and 3.2, design control input u_i for vehicle i , $i \in \{1, \dots, n\}$, based only on the bearing measurements $\{-g_{i-1}, g_i\}$ such that θ_i converges to θ_i^* in finite time. During the formation evolution, collision avoidance between any vehicles (no matter they are neighbours or not) should be guaranteed.

3.2 Proposed control law

We next propose a control law to solve Problem 3.3. Define the *angle error* for vehicle i as

$$\varepsilon_i = \cos \theta_i - \cos \theta_i^* = -g_i^T g_{i-1} - \cos \theta_i^*, \quad (8)$$

where the second equality is due to $-g_i^T g_{i-1} = \|g_i\| \|g_{i-1}\| \cos \theta_i = \cos \theta_i$. The proposed control law for vehicle i is

$$u_i = \text{sgn}(\varepsilon_i)(g_i - g_{i-1}), \quad (9)$$

where

$$\text{sgn}(\varepsilon_i) = \begin{cases} 1 & \text{if } \varepsilon_i > 0 \\ 0 & \text{if } \varepsilon_i = 0. \\ -1 & \text{if } \varepsilon_i < 0 \end{cases}$$

For vector arguments, $\text{sgn}(\cdot)$ is defined component-wise. Inspired by the control law in Basiri et al. (2010), the proposed control law (9) has a clear geometric meaning: the control input vector u_i is along the bisector of the angle θ_i .

3.3 Error dynamics

We next derive the error dynamics of the closed-loop system under control law (9).

Denote $\varepsilon = [\varepsilon_1, \dots, \varepsilon_n]^T \in \mathbb{R}^n$. Recall g_i is defined as $g_i = e_i / \|e_i\|$. Then the time derivative of g_i is

$$\begin{aligned} \dot{g}_i &= \frac{\dot{e}_i}{\|e_i\|} - \frac{e_i}{\|e_i\|^2} \frac{d\|e_i\|}{dt} \\ &= \frac{1}{\|e_i\|} \left(I - \frac{e_i e_i^T}{\|e_i\|^2} \right) \dot{e}_i \\ &= \frac{1}{\|e_i\|} P_i \dot{e}_i, \end{aligned} \quad (10)$$

where $P_i = I - g_i g_i^T$. Matrix P_i plays an important role in the stability analysis in this paper. Geometrically, P_i is an orthogonal projection matrix which can orthogonally project any vector onto the orthogonal complement of g_i . The algebraic properties of P_i are listed as follows:

Lemma 3.4: *Matrix P_i satisfies:*

- (i) $P_i^T = P_i$ and $P_i^2 = P_i$.
- (ii) P_i is positive semi-definite.
- (iii) $\text{Null}(P_i) = \text{span}\{g_i\}$.

Proof:

- (i) The two properties are trivial to check.
- (ii) For any $x \in \mathbb{R}^2$, since $P_i^2 = P_i$ and $P_i^T = P_i$, we have $x^T P_i x = x^T P_i^T P_i x = \|P_i x\|^2 \geq 0$.
- (iii) First, it is easy to see $P_i g_i = 0$ and hence $g_i \in \text{Null}(P_i)$. Second, for any $x \in \mathbb{R}^2$, we have $P_i x = x - (g_i^T x) g_i$. Clearly $P_i x = 0$ only if x is parallel to g_i . Thus $\text{Null}(P_i) = \text{span}\{g_i\}$. □

Based on Equation (10), we obtain the dynamics of ε as follows:

Theorem 3.5: *The ε -dynamics under control law (9) is*

$$\dot{\varepsilon} = -A \text{sgn}(\varepsilon), \quad (11)$$

where $A \in \mathbb{R}^{n \times n}$, and all of the entries of A are zero except

$$\begin{aligned} [A]_{i(i-1)} &= \frac{1}{\|e_{i-1}\|} g_i^T P_{i-1} g_{i-2}, \\ [A]_{ii} &= \frac{1}{\|e_{i-1}\|} g_i^T P_{i-1} g_i + \frac{1}{\|e_i\|} g_{i-1}^T P_i g_{i-1}, \\ [A]_{i(i+1)} &= \frac{1}{\|e_i\|} g_{i-1}^T P_i g_{i+1}, \end{aligned} \quad (12)$$

for all $i \in \{1, \dots, n\}$.

Proof: Recall $e_i = z_{i+1} - z_i$. Then substituting control law (9) into $\dot{e}_i = \dot{z}_{i+1} - \dot{z}_i$ yields

$$\begin{aligned}\dot{e}_i &= \dot{z}_{i+1} - \dot{z}_i \\ &= \text{sgn}(\varepsilon_{i+1})(g_{i+1} - g_i) - \text{sgn}(\varepsilon_i)(g_i - g_{i-1}) \\ &= \text{sgn}(\varepsilon_{i+1})g_{i+1} + \text{sgn}(\varepsilon_i)g_{i-1} \\ &\quad - [\text{sgn}(\varepsilon_{i+1}) + \text{sgn}(\varepsilon_i)]g_i.\end{aligned}\quad (13)$$

Substituting Equation (13) into Equation (10) and using the fact that $P_i g_i = 0$ gives

$$\dot{g}_i = \frac{1}{\|e_i\|} P_i [\text{sgn}(\varepsilon_{i+1})g_{i+1} + \text{sgn}(\varepsilon_i)g_{i-1}].$$

Recall $\varepsilon_i = -g_i^T g_{i-1} - \cos \theta_i^*$ as defined in Equation (8) and θ_i^* is constant. Then by the above equation, we have

$$\begin{aligned}\dot{\varepsilon}_i &= -g_i^T \dot{g}_{i-1} - g_{i-1}^T \dot{g}_i \\ &= -\frac{1}{\|e_{i-1}\|} g_i^T P_{i-1} [\text{sgn}(\varepsilon_i)g_i + \text{sgn}(\varepsilon_{i-1})g_{i-2}] \\ &\quad - \frac{1}{\|e_i\|} g_{i-1}^T P_i [\text{sgn}(\varepsilon_{i+1})g_{i+1} + \text{sgn}(\varepsilon_i)g_{i-1}] \\ &= -[A]_{i(i-1)} \text{sgn}(\varepsilon_{i-1}) - [A]_{ii} \text{sgn}(\varepsilon_i) \\ &\quad - [A]_{i(i+1)} \text{sgn}(\varepsilon_{i+1}),\end{aligned}\quad (14)$$

where $[A]_{i(i-1)}$, $[A]_{ii}$ and $[A]_{i(i+1)}$ are given in Equation (12). It is straightforward to see the matrix form of Equation (14) is Equation (11). \square

We next prove that the matrix A in Equation (11) is symmetric positive semi-definite.

Corollary 3.6: *The matrix A in Equation (11) is symmetric positive semi-definite. For any $x = [x_1, \dots, x_n]^T \in \mathbb{R}^n$,*

$$\begin{aligned}x^T A x &= \sum_{i=1}^n \frac{1}{\|e_i\|} (g_{i+1} x_{i+1} + g_{i-1} x_i)^T \\ &\quad \times P_i (g_{i+1} x_{i+1} + g_{i-1} x_i) \geq 0.\end{aligned}\quad (15)$$

Proof: To prove A is symmetric, we only need to prove $[A]_{(i+1)i} = [A]_{i(i+1)}$ for all i . By changing the index i in $[A]_{i(i-1)}$ in Equation (12) to $i+1$, we obtain

$$[A]_{(i+1)i} = \frac{1}{\|e_i\|} g_{i+1}^T P_i g_{i-1}.$$

It is clear that $[A]_{(i+1)i} = [A]_{i(i+1)}$ due to the symmetry of P_i . For any vector $x = [x_1, \dots, x_n]^T \in \mathbb{R}^n$, we have

$$\begin{aligned}x^T A x &= \sum_{i=1}^n [A]_{i(i-1)} x_i x_{i-1} + [A]_{ii} x_i^2 + [A]_{i(i+1)} x_i x_{i+1} \\ &= \sum_{i=1}^n \left(\frac{1}{\|e_{i-1}\|} g_i^T P_{i-1} g_{i-2} \right) x_i x_{i-1}\end{aligned}$$

$$\begin{aligned}&+ \sum_{i=1}^n \left(\frac{1}{\|e_{i-1}\|} g_i^T P_{i-1} g_i \right) x_i^2 \\ &+ \sum_{i=1}^n \left(\frac{1}{\|e_i\|} g_{i-1}^T P_i g_{i-1} \right) x_i^2 \\ &+ \sum_{i=1}^n \left(\frac{1}{\|e_i\|} g_{i-1}^T P_i g_{i+1} \right) x_i x_{i+1} \\ &= \sum_{i=1}^n \left(\frac{1}{\|e_i\|} g_{i+1}^T P_i g_{i-1} \right) x_{i+1} x_i \\ &+ \sum_{i=1}^n \left(\frac{1}{\|e_i\|} g_{i+1}^T P_i g_{i+1} \right) x_{i+1}^2 \\ &+ \sum_{i=1}^n \left(\frac{1}{\|e_i\|} g_{i-1}^T P_i g_{i-1} \right) x_i^2 \\ &+ \sum_{i=1}^n \left(\frac{1}{\|e_i\|} g_{i-1}^T P_i g_{i+1} \right) x_i x_{i+1} \\ &= \sum_{i=1}^n \frac{1}{\|e_i\|} (g_{i+1} x_{i+1} + g_{i-1} x_i)^T \\ &\quad \times P_i (g_{i+1} x_{i+1} + g_{i-1} x_i) \geq 0,\end{aligned}$$

where the last inequality is due to the fact that P_i is positive semi-definite. \square

4. Formation stability analysis

In this section, we analyse the stability of the error dynamics (11). By employing a locally Lipschitz Lyapunov function and the nonsmooth analysis tools introduced in Section 2.3, we prove that the origin $\varepsilon = 0$ is locally finite-time stable with collision avoidance guaranteed. In addition to the dynamics of ε , we also analyse the behaviours of the vehicle positions during formation evolution.

We first consider the problem of collision avoidance. On one hand, Assumption 3.1 states that no vehicles coincide with each other in the initial formation, i.e. $z_i(0) \neq z_j(0)$ for any $i \neq j$. On the other hand, control law (9) implies that $\|\dot{z}_i\| \leq \|g_i - g_{i-1}\| \leq 2$, which means that the maximum speed of each vehicle is two. Therefore, any two vehicles are not able to collide with each other (no matter they are neighbours or not) for all $t \in [0, T^*)$ where

$$T^* \triangleq \frac{\min_{i \neq j} \|z_i(0) - z_j(0)\|}{4}.$$

In the rest of the paper, we will only consider $t \in [0, T]$ with $T < T^*$. We will prove that the system can be stabilised within the finite time interval $[0, T]$.

Consider the Lyapunov function,

$$V(\varepsilon) = \sum_{i=1}^n |\varepsilon_i|, \quad (16)$$

which is positive definite in ε . Note $V(\varepsilon)$ is locally Lipschitz and convex. Hence $V(\varepsilon)$ is also regular.

Theorem 4.1: For the error dynamics (11) and Lyapunov function (16), the Filippov differential inclusion is $\dot{\varepsilon} \in -A\partial V(\varepsilon)$. The set-valued Lie derivative is given by

$$\begin{aligned} \tilde{\mathcal{L}}_{-A\partial V} V(\varepsilon) = \{ \ell \in \mathbb{R} \mid \exists \eta \in \partial V(\varepsilon), \forall \zeta \in \partial V(\varepsilon), \\ -\zeta^T A \eta = \ell \}. \end{aligned} \quad (17)$$

When $\tilde{\mathcal{L}}_{-A\partial V} V(\varepsilon) \neq \emptyset$, for any $\ell \in \tilde{\mathcal{L}}_{-A\partial V} V(\varepsilon)$, there exists $\eta \in \partial V(\varepsilon)$ such that

$$\ell = -\eta^T A \eta \leq 0. \quad (18)$$

Proof: Step 1: calculate the generalised gradient. By definition, we have the generalised gradient as

$$\begin{aligned} \partial V(\varepsilon) = \{ \eta = [\eta_1, \dots, \eta_n]^T \in \mathbb{R}^n \mid \eta_i = \text{sgn}(\varepsilon_i) \text{ if } \varepsilon_i \neq 0 \\ \text{and } \eta_i \in [-1, 1] \text{ if } \varepsilon_i = 0 \text{ for } i \in \{1, \dots, n\} \}. \end{aligned}$$

Because $|\eta_i| = |\text{sgn}(\varepsilon_i)| = 1$ if $\varepsilon_i \neq 0$, we have the obvious but important fact that

$$\|\eta\| \geq 1, \quad \forall \eta \in \partial V(\varepsilon), \quad \forall \varepsilon \neq 0. \quad (19)$$

Additionally, if $\varepsilon_i \neq 0$, then $\text{Ln}(\{\text{sgn}(\varepsilon_i)\}) = \{\text{sgn}(\varepsilon_i)\}$; and if $\varepsilon_i = 0$, then $\text{Ln}([-1, 1]) = \{0\} = \{\text{sgn}(0)\}$. Thus we have the following useful property:

$$\text{Ln}(\partial V(\varepsilon)) = \{\text{sgn}(\varepsilon)\}. \quad (20)$$

Step 2: calculate the Filippov differential inclusion. Since $\|e_i(t)\| \neq 0$ for all i and all $t \in [0, T]$, the matrix A in Equation (9) is continuous. Then by Paden and Sastri (1987, Theorem 1), the Filippov differential inclusion associated with the system (11) can be calculated as

$$\dot{\varepsilon} \in \mathcal{F}[-A\text{sgn}(\varepsilon)] = -A\mathcal{F}[\text{sgn}(\varepsilon)]. \quad (21)$$

Substituting Equation (20) into Equation (21) yields

$$\mathcal{F}[\text{sgn}(\varepsilon)] = \mathcal{F}[\text{Ln}(\partial V(\varepsilon))] = \partial V(\varepsilon),$$

where the last equality uses the fact (5). Thus the Filippov differential inclusion in Equation (21) can be rewritten as

$$\dot{\varepsilon} \in -A\partial V(\varepsilon). \quad (22)$$

Step 3: calculate the set-valued Lie derivative. The set-valued Lie derivative of $V(\varepsilon)$ with respect to Equation (22) is given by

$$\begin{aligned} \tilde{\mathcal{L}}_{-A\partial V} V(\varepsilon) \\ = \{ \ell \in \mathbb{R} \mid \exists \xi \in -A\partial V(\varepsilon), \forall \zeta \in \partial V(\varepsilon), \zeta^T \xi = \ell \} \\ = \{ \ell \in \mathbb{R} \mid \exists \eta \in \partial V(\varepsilon), \forall \zeta \in \partial V(\varepsilon), -\zeta^T A \eta = \ell \}. \end{aligned}$$

The set $\tilde{\mathcal{L}}_{-A\partial V} V(\varepsilon)$ could be empty. When $\tilde{\mathcal{L}}_{-A\partial V} V(\varepsilon) \neq \emptyset$, for any $\ell \in \tilde{\mathcal{L}}_{-A\partial V} V(\varepsilon)$, there exists $\eta \in \partial V$ such that $\ell = -\zeta^T A \eta$ for all $\zeta \in \partial V$. In particular, by choosing $\zeta = \eta$, we have $\ell = -\eta^T A \eta \leq 0$. Note $-\eta^T A \eta \leq 0$ is due to the fact that A is a positive semi-definite matrix as shown in Lemma 3.6. Therefore, we have either $\tilde{\mathcal{L}}_{-A\partial V} V(\varepsilon) = \emptyset$ or $\max \tilde{\mathcal{L}}_{-A\partial V} V(\varepsilon) \leq 0$. \square

4.1 Main stability result

We first introduce a number of useful results and then prove the local finite-time formation stability.

Given an angle $\alpha \in \mathbb{R}$ and a vector $x \in \mathbb{R}^2$, the angle between x and $R(\alpha)x$ is α . Thus for all nonzero $x \in \mathbb{R}^2$, $x^T R(\alpha)x > 0$ when $\alpha \in (-\pi/2, \pi/2) \pmod{2\pi}$; $x^T R(\alpha)x = 0$ when $\alpha = \pm\pi/2 \pmod{2\pi}$ and $x^T R(\alpha)x < 0$ when $\alpha \in (\pi/2, 3\pi/2) \pmod{2\pi}$.

Lemma 4.2: Let $g_i^\perp \triangleq R(\pi/2)g_i$. The properties of g_i^\perp are listed as follows:

- (i) $\|g_i^\perp\| = 1$ and $(g_i^\perp)^T g_i = 0$.
- (ii) $P_i = g_i^\perp (g_i^\perp)^T$.
- (iii) For $i \neq j$, $(g_i^\perp)^T g_j = -(g_j^\perp)^T g_i$.
- (iv) $(g_i^\perp)^T g_{i-1} = \sin \theta_i$, which implies $(g_i^\perp)^T g_{i-1} > 0$ if $\theta_i \in (0, \pi)$; and $(g_i^\perp)^T g_{i-1} < 0$ if $\theta_i \in (\pi, 2\pi)$.

Proof: See Appendix. \square

Lemma 4.3: Let $\mathcal{U} \triangleq \{x \in \mathbb{R}^n : x \neq 0 \text{ and nonzero entries of } x \text{ do not have the same sign}\}$. Suppose $B \in \mathbb{R}^{n \times n}$ is a symmetric positive semi-definite matrix with $\lambda_1(B) = 0$ and $\lambda_2(B) > 0$. If $\mathbf{1} = [1, \dots, 1]^T \in \mathbb{R}^n$ is an eigenvector associated with the zero eigenvalue of B , then

$$\inf_{x \in \mathcal{U}} \frac{x^T B x}{x^T x} = \frac{\lambda_2(B)}{n}.$$

Proof: See Appendix.

Remark 2: By the definition of \mathcal{U} , any $x \in \mathcal{U}$ should at least contain one positive entry and one negative entry. If the nonzero entries of x are all positive or negative, then $x \notin \mathcal{U}$.

With the above preparation, we are ready to prove the formation stability based on Theorem 4.1. Note if $\tilde{\mathcal{L}}_{-A\partial V} V(\varepsilon) = \emptyset$, we have $\max \tilde{\mathcal{L}}_{-A\partial V} V(\varepsilon) = -\infty$ (see Section 2.3.3). Hence we need only to focus on the case of $\tilde{\mathcal{L}}_{-A\partial V} V(\varepsilon) \neq \emptyset$.

Theorem 4.4: Consider the set-valued Lie derivative given in Equation (17). When $\tilde{\mathcal{L}}_{-A\partial V} V(\varepsilon) \neq \emptyset$, for any $\ell \in \tilde{\mathcal{L}}_{-A\partial V} V(\varepsilon)$, there exists $\eta \in \partial V(\varepsilon)$ such that

$$\ell \leq -\frac{1}{\sum_{i=1}^n \|e_i\|} \eta^T D^T E^T E D \eta, \quad (23)$$

where

$$E = \begin{bmatrix} 1 & -1 & 0 & \dots & 0 \\ 0 & 1 & -1 & \dots & 0 \\ 0 & 0 & 1 & \dots & 0 \\ \vdots & \vdots & \vdots & \ddots & \vdots \\ -1 & 0 & \dots & 0 & 1 \end{bmatrix} \in \mathbb{R}^{n \times n},$$

$$D = \begin{bmatrix} (g_1^\perp)^\top g_n & 0 & 0 & \dots & 0 \\ 0 & (g_2^\perp)^\top g_1 & 0 & \dots & 0 \\ 0 & 0 & (g_3^\perp)^\top g_2 & \dots & 0 \\ \vdots & \vdots & \vdots & \ddots & \vdots \\ 0 & 0 & \dots & 0 & (g_n^\perp)^\top g_{n-1} \end{bmatrix} \in \mathbb{R}^{n \times n}. \tag{24}$$

Proof: By Equation (15), we can rewrite $\ell = -\eta^\top A \eta$ in Equation (18) as

$$\begin{aligned} \ell &= -\sum_{i=1}^n \frac{1}{\|e_i\|} (g_{i+1} \eta_{i+1} + g_{i-1} \eta_i)^\top P_i (g_{i+1} \eta_{i+1} + g_{i-1} \eta_i) \\ &\leq -\frac{1}{\sum_{i=1}^n \|e_i\|} \sum_{i=1}^n (g_{i+1} \eta_{i+1} + g_{i-1} \eta_i)^\top \\ &\quad \times P_i (g_{i+1} \eta_{i+1} + g_{i-1} \eta_i) \\ &= -\frac{1}{\sum_{i=1}^n \|e_i\|} \sum_{i=1}^n [(g_{i+1} \eta_{i+1} + g_{i-1} \eta_i)^\top g_i^\perp]^2 \\ &\quad \text{(By Lemma 4.2 (ii))} \\ &= -\frac{1}{\sum_{i=1}^n \|e_i\|} \sum_{i=1}^n [(g_i^\perp)^\top g_{i+1} \eta_{i+1} + (g_i^\perp)^\top g_{i-1} \eta_i]^2 \\ &= -\frac{1}{\sum_{i=1}^n \|e_i\|} h^\top h, \end{aligned} \tag{25}$$

where

$$\begin{aligned} h &= \begin{bmatrix} (g_1^\perp)^\top g_2 \eta_2 + (g_1^\perp)^\top g_n \eta_1 \\ \vdots \\ (g_n^\perp)^\top g_1 \eta_1 + (g_n^\perp)^\top g_{n-1} \eta_n \end{bmatrix} \\ &= \begin{bmatrix} (g_1^\perp)^\top g_n & (g_1^\perp)^\top g_2 & 0 & \dots & 0 \\ 0 & (g_2^\perp)^\top g_1 & (g_2^\perp)^\top g_3 & \dots & 0 \\ 0 & 0 & (g_3^\perp)^\top g_2 & \dots & 0 \\ \vdots & \vdots & \vdots & \ddots & \vdots \\ (g_n^\perp)^\top g_1 & 0 & \dots & 0 & (g_n^\perp)^\top g_{n-1} \end{bmatrix} \begin{bmatrix} \eta_1 \\ \eta_2 \\ \eta_3 \\ \vdots \\ \eta_n \end{bmatrix} \\ &= ED\eta, \end{aligned} \tag{26}$$

with E and D given in Equation (24). The last equality of Equation (26) uses the fact that $(g_i^\perp)^\top g_{i-1} = -(g_{i-1}^\perp)^\top g_i$ as

shown in Lemma 4.2 (iii). Substituting Equation (26) into Equation (25) gives Equation (23). \square

Note that D is a diagonal matrix and E actually is an incidence matrix of a directed and connected cycle graph. We now present the main stability result.

Theorem 4.5: *Under Assumptions 3.1 and 3.2, the equilibrium $\varepsilon = 0$ of system (11) is locally finite-time stable. Collision avoidance between any vehicles (no matter they are neighbours or not) can be locally guaranteed.*

Proof: Consider the time interval $[0, T]$ with $T < T^*$. Then $\|e_i(t)\| \neq 0$ and $\|e_i(t)\| \neq +\infty$ for all $t \in [0, T]$. We will prove that ε can converge to zero in the finite time interval $[0, T]$ if $\varepsilon(0)$ is sufficiently small.

Let $\Omega(\varepsilon(0)) \triangleq \{\varepsilon \in \mathbb{R}^n \mid V(\varepsilon) \leq V(\varepsilon(0))\}$. Since $V(\varepsilon) = \sum_{i=1}^n |\varepsilon_i| = \|\varepsilon\|_1$, the level set $\Omega(\varepsilon(0))$ is connected and compact. Because $\tilde{\mathcal{L}}_{-A\partial V} V(\varepsilon) = \emptyset$ or $\max \tilde{\mathcal{L}}_{-A\partial V} V(\varepsilon) \leq 0$ for any $\varepsilon \in \Omega(\varepsilon(0))$ as proved in Theorem 4.1, we have that $\Omega(\varepsilon(0))$ is strongly invariant to Equation (11) over $[0, T]$ by Lemma 2.1.

Step 1: prove the nonzero entries of $D\eta$ do not have the same sign.

Denote $\delta_i = \theta_i - \theta_i^*$ and $\delta = [\delta_1, \dots, \delta_n]^\top \in \mathbb{R}^n$. Consider the case of $\varepsilon \neq 0$ and hence $\delta \neq 0$. Because $\sum_{i=1}^n \theta_i \equiv \sum_{i=1}^n \theta_i^*$, we have $\sum_{i=1}^n \delta_i \equiv 0$. Thus the nonzero entries of δ do not have the same sign if $\delta \neq 0$. Let

$$w_i \triangleq \frac{\cos \theta_i - \cos \theta_i^*}{\theta_i - \theta_i^*}.$$

Then $\varepsilon_i = w_i \delta_i$, and hence

$$\varepsilon = W\delta,$$

where $W = \text{diag}\{w_1, \dots, w_n\} \in \mathbb{R}^{n \times n}$. Since $\lim_{\theta_i \rightarrow \theta_i^*} w_i = -\sin \theta_i^*$ by L'Hôpital's rule, the equations $\varepsilon_i = w_i \delta_i$ and $\varepsilon = W\delta$ are always valid even when $\theta_i - \theta_i^* = 0$.

Suppose $V(\varepsilon(0))$ is sufficiently small such that $\theta_i(0)$ is sufficiently close to θ_i^* and hence $\theta_i, \theta_i^* \in (0, \pi)$ or $\theta_i, \theta_i^* \in (\pi, 2\pi)$ for all $\varepsilon \in \Omega(\varepsilon(0))$. Then it is easy to see that $w_i < 0$ if $\theta_i, \theta_i^* \in (0, \pi)$, and $w_i > 0$ if $\theta_i, \theta_i^* \in (\pi, 2\pi)$. On the other hand, recall $(g_i^\perp)^\top g_{i-1} > 0$ when $\theta_i \in (0, \pi)$, and $(g_i^\perp)^\top g_{i-1} < 0$ when $\theta_i \in (\pi, 2\pi)$ as shown in Lemma 4.2 (iv). Thus we have

$$(g_i^\perp)^\top g_{i-1} w_i < 0,$$

for all $i \in \{1, \dots, n\}$. Since $[D]_{ii} = (g_i^\perp)^\top g_{i-1}$, the above inequality implies that the diagonal entries of DW have the same sign. Thus as the nonzero entries in δ do not have the same sign, the nonzero entries of $DW\delta = D\varepsilon$ do not have the same sign either. Furthermore, because $\eta_i = \text{sgn}(\varepsilon_i)$ if $\varepsilon_i \neq 0$, the nonzero entry ε_i has the same sign with η_i . As a

result, the nonzero entries of $D\eta$ do not have the same sign. Thus we have $D\eta \in \mathcal{U}$ with \mathcal{U} defined in Lemma 4.3.

Step 2: determine the negative upper bound of ℓ .

Note E is an incidence matrix of a directed and connected cycle graph. By Godsil and Royle (2001, Theorem 8.3.1), we have $\text{rank}(E) = n - 1$ and $\text{Null}(E^T E) = \text{Null}(E) = \text{span}\{\mathbf{1}\}$. Thus inequality (23) implies

$$\begin{aligned} \ell &\leq -\frac{1}{\sum_{i=1}^n \|e_i\|} \frac{\lambda_2(E^T E)}{n} \|D\eta\|^2 \quad (\text{By Lemma 4.3}) \\ &\leq -\frac{1}{\sum_{i=1}^n \|e_i\|} \frac{\lambda_2(E^T E)}{n} \lambda_1(D^2) \|\eta\|^2 \\ &\leq -\frac{1}{\sum_{i=1}^n \|e_i\|} \frac{\lambda_2(E^T E)}{n} \lambda_1(D^2), \end{aligned} \quad (27)$$

where the last inequality uses the fact $\|\eta\| \geq 1$ if $\varepsilon \neq 0$ as shown in Equation (19).

Now we analyse the two terms, $\sum_{i=1}^n \|e_i\|$ and $\lambda_1(D^2)$, in Equation (27). (1) Over the finite time interval $[0, T]$, the quantity $\sum_{i=1}^n \|e_i\|$ cannot go to infinity because the vehicle speed is finite. Hence there exists a constant $\gamma > 0$ such that $\sum_{i=1}^n \|e_i\| \leq \gamma$. (2) Since D is diagonal, we have $\lambda_1(D^2) = \min_i [D^2]_{ii}$. At the equilibrium point $\varepsilon = 0$ (i.e. $\theta_i = \theta_i^*$ for all i), we have $[D]_{ii} = (g_i^\perp)^T g_{i-1} \neq 0$ because $\theta_i^* \neq 0$ or π as stated in Assumption 3.2. By continuity, we can still have $[D]_{ii} \neq 0$ for all $\varepsilon \in \Omega(\varepsilon(0))$ if $\varepsilon(0)$ is sufficiently small. Because $\Omega(\varepsilon(0))$ is compact, there exists a lower bound β such that $\lambda_1(D^2) \geq \beta$ for all $\varepsilon \in \Omega(\varepsilon(0))$. By (1) and (2), inequality (27) can be rewritten as

$$\ell \leq -\frac{\beta \lambda_2(E^T E)}{\gamma n} \triangleq -\kappa < 0, \quad \forall \varepsilon \in \Omega(\varepsilon(0)) \setminus \{0\}. \quad (28)$$

Step 3: draw the stability conclusion.

If $\varepsilon = 0$ we have $0 \in \tilde{\mathcal{L}}_{-A\partial V} V(\varepsilon)$ because of Equation (17) and the fact that $0 \in \partial V(0)$; if $\varepsilon \neq 0$ we have $0 \notin \tilde{\mathcal{L}}_{-A\partial V} V(\varepsilon)$ because $\max \tilde{\mathcal{L}}_{-A\partial V} V(\varepsilon) < 0$ by Equation (28). Thus by the definition (6), we have

$$Z_{-\text{Asgn}(\varepsilon), V(\varepsilon)} = \{0\}. \quad (29)$$

Based on Equations (28) and (29) and Lemma 2.2, any solution of Equation (11) starting from $\varepsilon(0)$ converges to $\varepsilon = 0$ in finite-time, and the convergence time is upper bounded by $V(\varepsilon(0))/\kappa$. Thus if $V(\varepsilon(0))$ satisfies

$$\frac{V(\varepsilon(0))}{\kappa} < T < T^*, \quad (30)$$

then the system can be stabilised within the time interval $[0, T]$ during which collision avoidance between any vehicles can be guaranteed. \square

While the local formation stability is proved in Theorem 4.5, the convergence region of the equilibrium $\varepsilon = 0$ is

not given. We next give a sufficient condition on $\varepsilon(0)$ to guarantee the convergence and collision avoidance.

Corollary 4.6: Let $\Delta_i \triangleq \min\{\theta_i^*, |\theta_i^* - \pi|, 2\pi - \theta_i^*\}$ where $i \in \{1, \dots, n\}$. There exists ξ such that $0 < \xi < \min_i \Delta_i$. Let $\bar{\varepsilon}_i \triangleq \min\{|\cos(\theta_i^* + \xi) - \cos \theta_i^*|, |\cos(\theta_i^* - \xi) - \cos \theta_i^*|\}$, $\zeta \triangleq \min_i\{\theta_i^* - \xi, |\pi - \theta_i^*| - \xi, 2\pi - \theta_i^* - \xi\}$ and $\gamma \triangleq \sum_{i=1}^n \|e_i(0)\| + 4T$. Under Assumptions 3.1 and 3.2, the proposed control law guarantees the convergence of ε to 0 in $[0, T]$ with collision avoidance between any vehicles if

$$V(\varepsilon(0)) < \min \left\{ \min_i \bar{\varepsilon}_i, \frac{\sin^2 \zeta \lambda_2(E^T E)}{\gamma n} T \right\}. \quad (31)$$

Proof: The proof of Theorem 4.5 requires $\varepsilon(0)$ to be sufficiently small such that the following three conditions hold: (i) $\lambda_1(D^2) = \min_i [D^2]_{ii} > 0$ for all $\varepsilon \in \Omega(\varepsilon(0))$; (ii) θ_i^* and $\theta(t)$ for all $t \in [0, T]$ are both in $(0, \pi)$ or $(\pi, 2\pi)$; and (iii) $V(\varepsilon(0))/\kappa < T$. Note condition (iii) ensures the collision avoidance.

Step 1: analyse condition (i). Recall $[D]_{ii} = (g_i^\perp)^T g_{i-1} = \sin \theta_i$ as proved in Lemma 4.2. Hence $\min_i [D^2]_{ii} > 0$ if $\theta_i(t) \neq 0$ and $\theta_i(t) \neq \pi$ for all $t \in [0, T]$. Thus condition (i) implies condition (i).

Step 2: analyse condition (ii). Denote $\Delta_i \triangleq \min\{\theta_i^*, |\theta_i^* - \pi|, 2\pi - \theta_i^*\}$. There exists ξ such that $0 < \xi < \min_i \Delta_i$. Let $\bar{\varepsilon}_i \triangleq \min\{|\cos(\theta_i^* + \xi) - \cos \theta_i^*|, |\cos(\theta_i^* - \xi) - \cos \theta_i^*|\}$. Then we have the following sufficient condition: if $\varepsilon(0)$ satisfies

$$V(\varepsilon(0)) < \min_i \bar{\varepsilon}_i, \quad (32)$$

then condition (ii) holds. To see that, for any $j \in \{1, \dots, n\}$, we have $|\varepsilon_j(t)| \leq \sum_{i=1}^n |\varepsilon_i(t)| = V(\varepsilon(t)) \leq V(\varepsilon(0)) < \min_i \bar{\varepsilon}_i \leq \bar{\varepsilon}_j$. Thus $|\varepsilon_j(t)| < \bar{\varepsilon}_j$ for all $t \in [0, T]$. Since the cosine function is monotone in $(0, \pi)$ or $(\pi, 2\pi)$, we have $|\varepsilon_j(t)| < \bar{\varepsilon}_j \implies |\theta_j(t) - \theta_j^*| < \xi$ and hence condition (ii) holds. It should be noted $\bar{\varepsilon}_i \neq 0$ and hence the set of $\varepsilon(0)$ that satisfies Equation (32) is always nonempty.

Further define $\zeta \triangleq \min_i\{\theta_i^* - \xi, |\pi - \theta_i^*| - \xi, 2\pi - \theta_i^* - \xi\}$. Then $|\theta_j(t) - \theta_j^*| < \xi$ implies $\theta_j(t) > \zeta, |\pi - \theta_j(t)| > \zeta$ and $2\pi - \theta_j(t) > \zeta$ for all $t \in [0, T]$. Thus $[D^2]_{ii} = \sin^2 \theta_i > \sin^2 \zeta$. Hence we have $\beta = \sin^2 \zeta$, where β is the lower bound of $\lambda_1(D^2)$ as defined in the proof of Theorem 4.5.

Step 3: analyse condition (iii). We first identify an upper bound of $\sum_{i=1}^n \|e_i\|$. Since the speed of each vehicle is bounded above by two, it is easy to see $\sum_{i=1}^n \|e_i(t)\| \leq \sum_{i=1}^n \|e_i(0)\| + 4nT \triangleq \gamma$ for all $t \in [0, T]$. Therefore, we have κ defined in Equation (28) as

$$\kappa = \frac{\sin^2 \zeta \lambda_2(E^T E)}{\gamma n},$$

substituting which into Equation (30) yields

$$V(\varepsilon(0)) < \frac{\sin^2 \zeta \lambda_2(E^T E)}{\gamma n} T.$$

Therefore, if $V(\varepsilon(0))$ satisfies Equation (31), then the three conditions are satisfied. By Theorem 4.5, the convergence of ε and collision avoidance between any vehicles can be guaranteed. \square

Up to this point, the stability of the ε -dynamics has been proved. From control law (9), it is trivial to see that $\dot{z}_i = 0$ if $\varepsilon_i = 0$. Hence each vehicle will converge to a finite stationary final position within finite time. In addition, suppose the target formation is achieved at time $t_f < V(\varepsilon(0))/\kappa$. Since $\|\dot{z}_i\| \leq \|g_i - g_{i-1}\| \leq 2$, we have $\|z_i(t_f)$

$- z_i(0)\| \leq 2t_f \leq 2V(\varepsilon(0))/\kappa$. Therefore, the final converged position $z_i(t_f)$ will be very close to its initial position $z_i(0)$ if the initial angle error $\varepsilon(0)$ is sufficiently small. In other words, the final converged formation will not be far away from the initial formation given small initial angle errors.

5. Simulation results

In this section, we present simulation results to illustrate the preceding theoretical analysis. Figures 2, 3, 4 and 5, respectively, show the formation control of three, four, five and eight vehicles. Note the five point star shown in Figure 3 is not a normal polygon. However, these kinds of formations still have underlying graphs as cycles and hence can be stabilised by the proposed control law. As shown in the

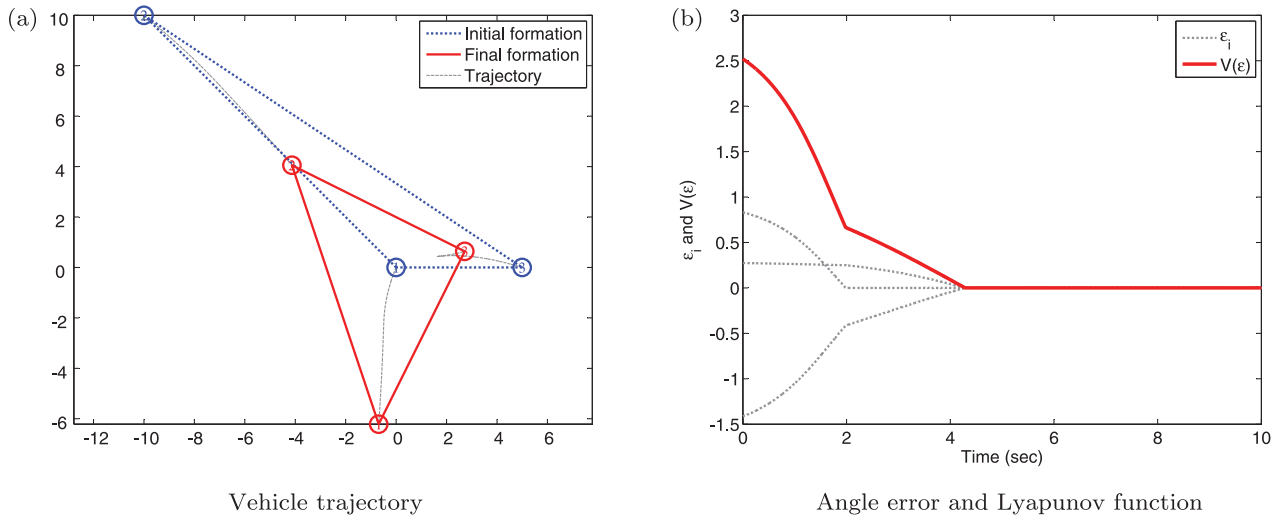


Figure 2. Control results by the proposed control law with $n = 3$, $\theta_1^* = \theta_2^* = 45\text{deg}$ and $\theta_3^* = 90\text{deg}$.

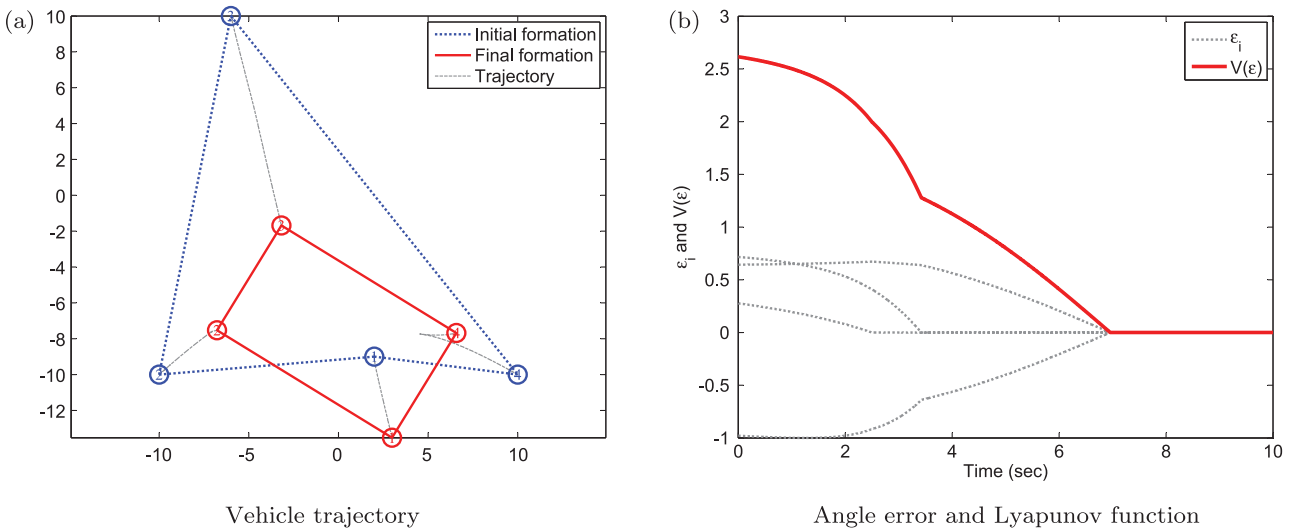


Figure 3. Control results by the proposed control law with $n = 4$ and $\theta_1^* = \dots = \theta_4^* = 90\text{deg}$.

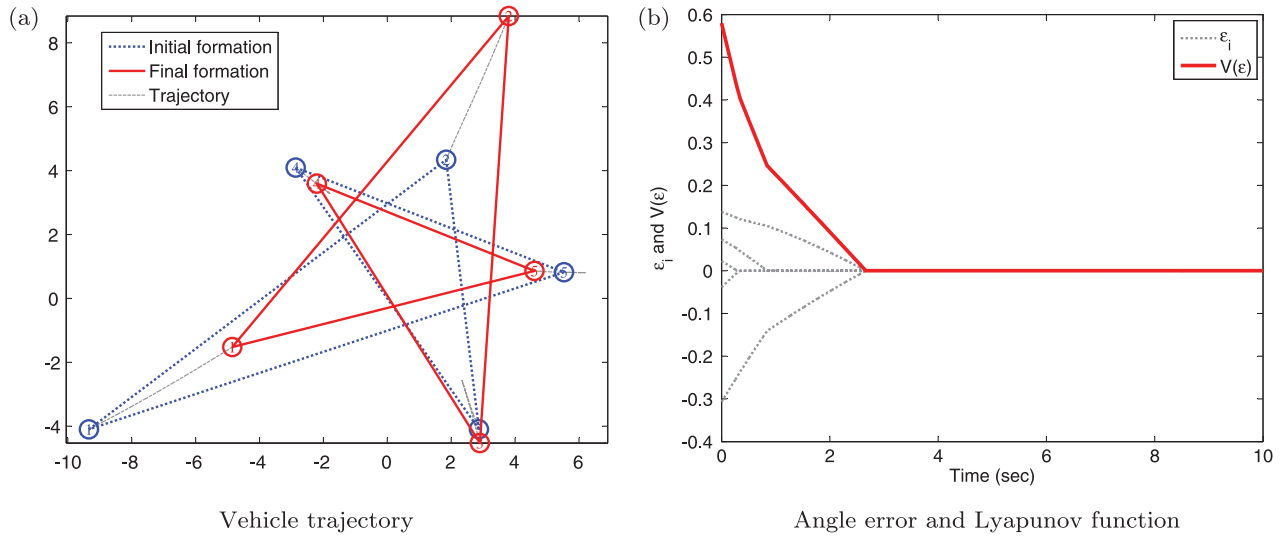


Figure 4. Control results by the proposed control law with $n = 5$ and $\theta_1^* = \dots = \theta_5^* = 36\text{deg}$.

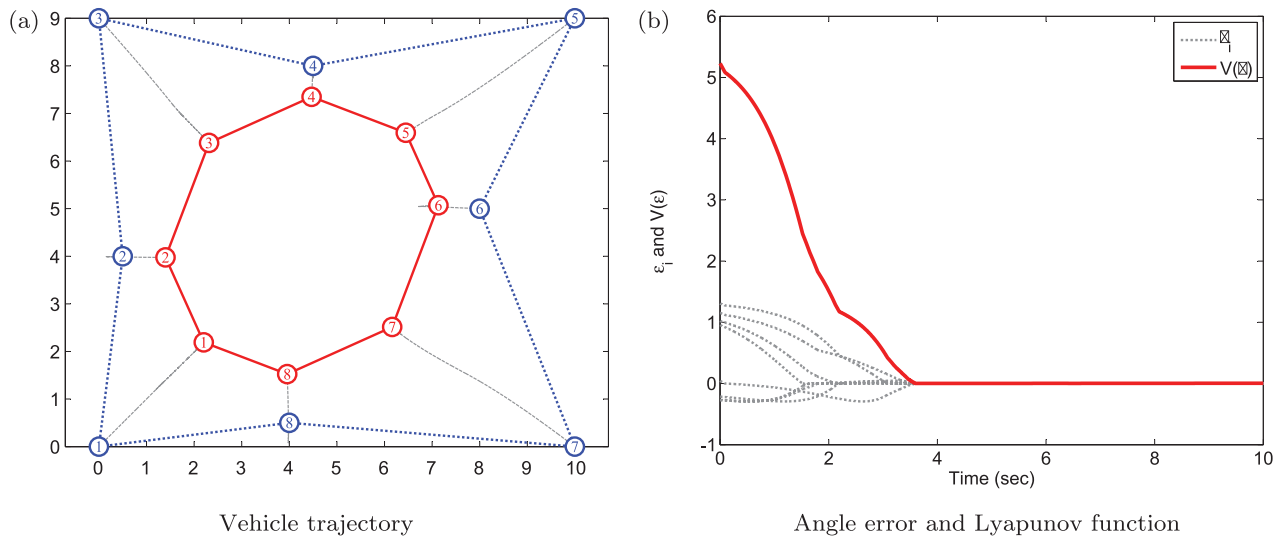


Figure 5. Control results by the proposed control law with $n = 8$ and $\theta_1^* = \dots = \theta_8^* = 135\text{deg}$.

simulation, the proposed control law can efficiently reduce the angle errors and stabilise the formation in finite time. In our stability proof, we assume that the initial angle error $\epsilon(0)$ should be sufficiently small such that $\theta_i(0)$ and θ_i^* are in either $(0, \pi)$ or $(\pi, 2\pi)$. However, as shown in Figures 3 and 5, the formation can still be stabilised even if $\theta_i(0)$ and θ_i^* may be, respectively, in the two intervals $(0, \pi)$ and $(\pi, 2\pi)$. Hence the simulation suggests that the attractive region of the target formation by the proposed control law is not necessarily small.

6. Conclusions

In this paper, we proposed a distributed control law to stabilise angle-constrained cyclic formations using bearing-only measurements. Compared to the existing work, the

proposed control law can handle cyclic formations with an arbitrary number of vehicles and only requires the sign information of the angle errors. By using nonsmooth stability analysis tools, we proved that the formation is locally finite-time stable with collision avoidance guaranteed.

Compared to the conventional position-based formation control, bearing-based formation control does possess a number of unique features. For example, the formation shape and the formation scale are uncontrollable by bearing-based formation control since the inter-vehicle distances are uncontrollable. However these limitations of bearing-based formation control can be all well overcome in the future. For example, the formation shape can be specified by assigning a rigid underlying graph to a formation. To control the scale of a formation, we can introduce some leader vehicles whose inter-vehicle distances are controllable. Then given

appropriate underlying sensing graph, the formation scale can be controlled by tuning the distances among the leader vehicles. These topics are very interesting and challenging directions for future research.

Here are some other interesting topics for future research on bearing-based formation control. First, this paper only considers formations with cycle graphs. One of our immediate research plans is to extend the work in this paper to the cases with more complicated graphs. The extension will be non-trivial, but the structure of the stability analysis in this paper is believed to be useful for future research on more complicated cases. Second, we assume the underlying graph is undirected in this paper. It may be more practical for the underlying sensing graphs to be directed. Finally, the vehicle dynamics is assumed as a single integrator in this work. More complicated vehicle dynamics and system uncertainties need to be considered in the future.

Note

1. In some literature such as Godsfil and Royle (2001), the rows of an incidence matrix are indexed by vertices and the columns are indexed by edges.

References

- Bacciotti, A., & Ceragioli, F. (1999). Stability and stabilization of discontinuous systems and nonsmooth Lyapunov functions. *ESAIM: Control, Optimisation and Calculus of Variations*, 4, 361–376.
- Basiri, M., Bishop, A.N., & Jensfelt, P. (2010). Distributed control of triangular formations with angle-only constraints. *Systems & Control Letters*, 59, 147–154.
- Bhat, S.P., & Bernstein, D.S. (2000). Finite-time stability of continuous autonomous systems. *SIAM Journal on Control and Optimization*, 38(3), 751–766.
- Bishop, A.N. (2011). Stabilization of rigid formations with direction-only constraints. In *Proceedings of the 50th IEEE Conference on Decision and Control and European Control Conference* (pp. 746–752). Orlando, FL.
- Cao, M., Yu, C., & Anderson, B.D.O. (2011). Formation control using range-only measurements. *Automatica*, 47, 776–781.
- Chen, G., Lewis, F.L., & Xie, L. (2011). Finite-time distributed consensus via binary control protocols. *Automatica*, 47, 1962–1968.
- Clarke, F.H. (1983). *Optimization and nonsmooth analysis*. New York, NY: Wiley.
- Cortés, J. (2008). Discontinuous dynamical systems. *IEEE Control Systems Magazine*, 28(3), 36–73.
- Cortés, J., & Bullo, F. (2005). Coordination and geometric optimization via distributed dynamical systems. *SIAM Journal on Control and Optimization*, 44(5), 1543–1574.
- Das, A.K., Fierro, R., Kumar, V., Ostrowski, J.P., Spletzer, J., & Taylor, C.J. (2002). A vision-based formation control framework. *IEEE Transactions on Robotics and Automation*, 18(5), 813–825.
- Dimarogonas, D.V., & Johansson, K.H. (2010). Stability analysis for multi-agent systems using the incidence matrix: Quantized communication and formation control. *Automatica*, 46(4), 695–700.
- Dörfler, F., & Francis, B. (2010). Geometric analysis of the formation problem for autonomous robots. *IEEE Transactions on Automatic Control*, 55(10), 2379–2384.
- Eren, T. (2012). Formation shape control based on bearing rigidity. *International Journal of Control*, 85(9), 1361–1379.
- Filippov, A.F. (1988). *Differential equations with discontinuous righthand sides*. Dordrecht: Kluwer Academic Publishers.
- Franchi, A., & Giordano, P.R. (2012). Decentralized control of parallel rigid formations with direction constraints and bearing measurements. In *Proceedings of the 51st IEEE Conference on Decision and Control* (pp. 5310–5317). Maui, HI.
- Godsil, C., & Royle, G. (2001). *Algebraic graph theory*. New York, NY: Springer.
- Hong, Y., Jiang, Z.P., & Feng, G. (2010). Finite-time input-to-state stability and applications to finite-time control design. *SIAM Journal on Control and Optimization*, 48(7), 4395–4418.
- Hong, Y., Xu, Y., & Huang, J. (2002). Finite-time control for robot manipulators. *Systems & Control Letters*, 46, 243–253.
- Hu, J., Xu, J., & Xie, L. (2013). Cooperative search and exploration in robotic networks. *Unmanned Systems*, 1(1), 121–142.
- Huang, H., Yu, C., & Wu, Q. (2013). Autonomous scale control of multiagent formations with only shape constraints. *International Journal of Robust and Nonlinear Control*, 23(7), 765–791.
- Keller, J., Thakur, D., Dobrokhodov, V., Jones, K., Pivtoraiko, M., Gallier, J., ... Kumar, V. (2013). A computationally efficient approach to trajectory management for coordinated aerial surveillance. *Unmanned Systems*, 1(1), 59–74.
- Kopeikin, A.N., Ponda, S.S., Johnson, L.B., & How, J.P. (2013). Dynamic mission planning for communication control in multiple unmanned aircraft teams. *Unmanned Systems*, 1(1), 41–58.
- Krick, L., Broucke, M.E., & Francis, B.A. (2009). Stabilization of infinitesimally rigid formations of multi-robot networks. *International Journal of Control*, 82(3), 423–439.
- Lin, Z., Francis, B., & Maggiore, M. (2005). Necessary and sufficient graphical conditions for formation control. *IEEE Transactions on Automatic Control*, 50(1), 121–127.
- Ma, Y., Soatto, S., Kosecka, J., & Sastry, S. (2004). *An invitation to 3D vision*. New York, NY: Springer.
- Mariottini, G.L., Morbidi, F., Prattichizzo, D., Valk, N.V., Michael, N., Pappas, G., & Daniilidis, K. (2009). Vision-based localization for leader–follower formation control. *IEEE Transactions on Robotics*, 25(6), 1431–1438.
- Meng, Z., & Lin, Z. (2012). Distributed finite-time cooperative tracking of networked lagrange systems via local interactions. In *Proceedings of American Control Conference* (pp. 4951–4956). Montreal, Canada.
- Moshtagh, N., Michael, N., Jadbabaie, A., & Daniilidis, K. (2008, June). *Bearing-only control laws for balanced circular formations of ground robots*. Paper presented at Proceedings of Robotics: Science and Systems, Zurich, Switzerland.
- Paden, B., & Sastry, S.S. (1987). A calculus for computing Filippovs differential inclusion with application to the variable structure control of robot manipulators. *IEEE Transactions on Circuits and Systems*, 34(1), 73–82.
- Ren, W., & Cao, Y. (2011). *Distributed coordination of multi-agent networks*. London: Springer-Verlag.
- Shevitz, D., & Paden, B. (1994). Lyapunov stability theory of nonsmooth systems. *IEEE Transactions on Automatic Control*, 39(9), 1910–1914.
- Tian, Y.-P., & Wang, Q. (2013). Global stabilization of rigid formations in the plane. *Automatica*, 49(5), 1436–1441.

Xiao, F., Wang, L., Chen, J., & Gao, Y. (2009). Finite-time formation control for multi-agent systems. *Automatica*, 45, 2605–2611.

Appendix

Proof [Proof of Lemma 4.2]:

- (i) The two equations are obvious.
- (ii) Denote $G_i = [g_i, g_i^\perp] \in \mathbb{R}^{2 \times 2}$. It is clear that G_i is an orthogonal matrix satisfying $G_i^T G_i = G_i G_i^T = I$. Hence we have

$$g_i g_i^T + g_i^\perp (g_i^\perp)^T = G_i G_i^T = I.$$

Thus $g_i^\perp (g_i^\perp)^T = I - g_i g_i^T = P_i$.

- (iii) $(g_i^\perp)^T g_j = g_i^T R^T(\pi/2) g_j = g_i^T R(-\pi/2) g_j = g_i^T R(-\pi) R(\pi/2) g_j = g_i^T R(-\pi) g_j^\perp = g_i^T (-I) g_j^\perp = -(g_j^\perp)^T g_i$.
- (iv) By the definition of θ_i , we have $g_i = R(\theta_i)(-g_{i-1})$ and hence $g_{i-1} = -R(-\theta_i)g_i$. Then

$$\begin{aligned} (g_i^\perp)^T g_{i-1} &= -g_i^T R\left(-\frac{\pi}{2}\right) R(-\theta_i)g_i \\ &= -g_i^T R\left(-\frac{\pi}{2} - \theta_i\right) g_i \\ &= -\|g_i\| \left\| R\left(-\frac{\pi}{2} - \theta_i\right) g_i \right\| \cos\left(-\frac{\pi}{2} - \theta_i\right) \\ &= \sin \theta_i. \end{aligned}$$

Then it is straightforward to see the rest of the results in Lemma 4.2 (iv). □

Proof [Proof of Lemma 4.3]: By orthogonally projecting $x \in \mathcal{U}$ to $\mathbf{1}$ and the orthogonal complement of $\mathbf{1}$, we decompose x as

$$x = x_0 + x_1,$$

where $x_0 \in \text{Null}(B)$ and $x_1 \perp \text{Null}(B)$. Let φ be the angle between $\mathbf{1}$ and x . Then we have

$$\begin{aligned} x^T B x &= x_1^T B x_1 \\ &\geq \lambda_2(B) \|x_1\|^2 \\ &= \lambda_2(B) \sin^2 \varphi \|x\|^2. \end{aligned} \tag{A.1}$$

By the definition of \mathcal{U} , any x in \mathcal{U} would not be in $\text{span}\{\mathbf{1}\}$. That means $\varphi \neq 0$ or π and hence $\sin \varphi \neq 0$. We next identify the positive infimum of $\sin \varphi$. The open set \mathcal{U} is enclosed by the hyper-planes $[x]_i = 0$ with $i \in \{1, \dots, n\}$. And $\mathbf{1}$ is isolated from any $x \in \mathcal{U}$ by the hyper-planes. Denote the boundary of \mathcal{U} as $\partial \mathcal{U}$. Then we have $\inf_{x \in \mathcal{U}} \varphi = \min_{x \in \partial \mathcal{U}} \angle(x, \mathbf{1})$ and $\sup_{x \in \mathcal{U}} \varphi = \max_{x \in \partial \mathcal{U}} \angle(x, \mathbf{1})$. Denote $p_i \in \mathbb{R}^n$ as the orthogonal projection of $\mathbf{1}$ on the hyper-plane $[x]_i = 0$. Then $\min_{x \in \partial \mathcal{U}} \angle(x, \mathbf{1}) = \angle(p_i, \mathbf{1})$ and $\max_{x \in \partial \mathcal{U}} \angle(x, \mathbf{1}) = \angle(-p_i, \mathbf{1})$. Note the i th entry of p_i is zero and the others are one. It can be calculated that $\cos \angle(\pm p_i, \mathbf{1}) = \pm \sqrt{n-1}/\sqrt{n}$ and hence $\sin \angle(\pm p_i, \mathbf{1}) = 1/\sqrt{n}$. Thus

$$\inf_{x \in \mathcal{U}} \sin \varphi = \frac{1}{\sqrt{n}},$$

substituting which into Equation (A.1) yields

$$\inf_{x \in \mathcal{U}} \frac{x^T B x}{x^T x} = \frac{\lambda_2(B)}{n}.$$

□